# Dimers Generated from Tetrameric Phosphorylating Glyceraldehyde-3-phosphate Dehydrogenase from *Bacillus stearothermophilus* Are Inactive but Exhibit Cooperativity in NAD Binding†

Olivier Roitel, Eduard Sergienko,‡ and Guy Branlant*

*Maturation des ARN et Enzymologie Moléculaire, Faculté des Sciences, UMR 7567 CNRS-UHP, B.P. 239, 54506 Vandoeuvre-les-Nancy Cédex, France*

*Received June 4, 1999; Revised Manuscript Received September 28, 1999*

ABSTRACT: Tetrameric phosphorylating glyceraldehyde-3-phosphate dehydrogenase (GAPDH) from *Bacillus stearothermophilus* has been described as a "dimer of dimers" with three nonequivalent interfaces, *P*-axis (between subunits O and P and between subunits Q and R), *Q*-axis (between subunits O and Q and between subunits P and R), and *R*-axis interface (between subunits O and R and between subunits P and Q). *O*−*P* dimers, the most stable and the easiest to generate, have been created by selective disruption of hydrogen bonds across the *R*- and *Q*-axis interfaces by site-directed mutagenesis. Asp-186 and Ser-48, and Glu-276 and Tyr-46, which are hydrogen bond partners across the *R*- and *Q*-axis interfaces, respectively, have been replaced with glycine residues. All mutated residues are highly conserved among GAPDHs from different species and are located in loops. Both double mutants D186G/E276G and Y46G/S48G were dimeric, while all single mutants remained tetrameric. As previously described [Clermont, S., Corbier, C., Mely, Y., Gerard, D., Wonacott, A., and Branlant, G. (1993) *Biochemistry 32*, 10178−10184], NAD binding to wild type GAPDH (wtGAPDH) was interpreted according to the induced-fit model and exhibited negative cooperativity. However, NAD binding to wtGAPDH can be adequately described in terms of two independent dimers with two interacting binding sites in each dimer. Single mutants D186G, E276G, and Y46G exhibited behavior in NAD binding similar to that of the wild type, while both dimeric mutants D186G/E276G and Y46G/S48G exhibited positive cooperativity in binding the coenzyme NAD. The fact that *O*−*P* dimer mutants retained cooperative behavior shows that (1) the *P*-axis interface is important in transmitting the information induced upon NAD binding inside the *O*−*P* dimer from one subunit to the other and (2) the S-loop of the *R*-axis-related subunit is not directly involved in cooperative binding of NAD in the *O*−*P* dimer. In both *O*−*P* dimer mutants, the absorption band of the binary enzyme−NAD complex had a highly decreased intensity compared to that of the wild type and, in addition, totally disappeared in the presence of G3P or 1,3-dPG. However, no enzymatic activity was detected, indicating that the formed ternary enzyme−NAD−G3P or −1,3-dPG complex was not catalytically efficient. In the *O*−*P* dimers, the interaction with the S-loop of the *R*-axis-related subunit is disrupted, and therefore, the S-loop should be less structured. This resulted in increased accessibility of the active site to the solvent, particularly for the adenosine-binding site of NAD. Thus, together, this is likely to explain both the lowered affinity of the dimeric enzyme for NAD and the absence of activity.

Many enzymes exist as oligomers of identical subunits. Among these oligomeric enzymes, dimers and tetramers are the most common species (*1*). While each subunit has only a single recognition site for a like subunit within a dimer, the existence of a second set of bonding sites leads to the formation of a tetramer. The main advantages of the oligomeric state have usually been described as improved stability of the enzyme and regulation of the enzymatic activity through interaction between subunits (*2*, *3*). To determine the role of the quaternary structure, properties of dissociated oligomeric enzymes have been studied. Two different approaches are utilized to dissociate oligomeric enzymes. The first approach consists of varying different physicochemical parameters such as pressure, temperature, pH, ionic strength, or concentration of effectors. The second approach, which was utilized in this study, is based on the known three-dimensional structure and molecular modeling for identifying and site-directed mutagenesis for characterizing the residues implied in intersubunit stabilizing interactions.

Only a minority of the oligomeric enzymes composed of identical subunits exhibit cooperative behavior (*1*). Many of the concepts of cooperative interactions come from studies on tetrameric phosphorylating GAPDHs.[1] Coenzyme binding to GAPDH was shown to exhibit either positive or negative cooperativity, depending on the source of the enzyme. Yeast

† This research was supported by the Centre National de la Recherche Scientifique and the University Henri Poincaré Nancy I.

* To whom all correspondence should be addressed. Phone: 33 3 83 91 20 97. Fax: 33 3 83 91 20 93. E-mail: guy.branlant@maem.uhp-nancy.fr.

‡ Present address: Department of Chemistry, Rutgers, the State University of New Jersey, Newark, NJ 07102.

10.1021/bi9912802 CCC: $18.00 
Published on Web 11/11/1999

GAPDH binds NAD with positive cooperativity at 40 °C and pH 8.5 (*4*), while GAPDHs isolated from rabbit (*5*, *6*), sturgeon (*7*, *8*), and lobster (*9*) muscles, *Escherichia coli* (*10*), and *Bacillus stearothermophilus* (*11*, *12*) exhibited negative cooperativity in binding the coenzyme NAD. Several models have been proposed to explain cooperative ligand binding to an oligomeric protein. The concerted model of Monod, Wyman, and Changeux (*13*) is only consistent with positive cooperativity. Two other models have been proposed to describe both negative and positive cooperativity. In the preexisting asymmetry model (*14*, *15*), symmetric and asymmetric quaternary conformations of the protein are in equilibrium. The character of cooperativity is explained as a result of the relative presence and affinities of the states. Alternatively, in the induced-fit model (*16*), enzymes both unligated and fully ligated with NAD are symmetric. NAD binding to the first subunit induces conformational changes that extend to subunit interfaces and affect the affinity of the neighboring subunit for NAD. Several studies on sturgeon GAPDH in solution (*7*, *8*) have been satisfactorily interpreted according to the preexisting asymmetry model asssumptions, whereas those on GAPDH from *B. stearothermophilus* (*11*, *17*) supported the induced-fit model.

*B. stearothermophilus* GAPDH reversibly catalyzes the oxidative phosphorylation of D-glyceraldehyde 3-phosphate (G3P) to 1,3-diphosphoglycerate (1,3-dPG) in the presence of NAD and inorganic phosphate ($P_i$) (*18*). As all other GAPDHs with known crystallographic structures, *B. stearothermophilus* GAPDH is a homotetramer with 222 symmetry. In other words, the tetramer could be described as a dimer of dimers (Figure 1) with three nonequivalent interfaces (*19*, *20*). The *P*-axis interface (between subunits O and P and between subunits Q and R) is the most extended interface (2400 Å$^2$) (*20*). The *R*-axis interface (between subunits O and R and between subunits P and Q) is smaller (1700 Å$^2$) (*20*). Finally, the *Q*-axis interface (between subunits O and Q and between subunits P and R) extends only through 600 Å$^2$ (*20*). The most extensive intersubunit interactions are formed by the *P*-axis-related monomers, with 48 residues per subunit containing atoms less than 4 Å from an atom in the adjoining subunit (*19*). There are 26 such residues per subunit in the *R*-axis-related subunits and only nine in the *Q*-axis interface. Molecular modeling of the three possible dimers showed that a total number of 222, 245, 286, and 300 hydrophobic residues (*21*) are exposed to the solvent in the wild type tetramer, *O*−*P* dimer, *O*−*R* dimer, and *O*−*Q* dimer, respectively. Therefore, because of the strength of the *P*-axis interface and of the lowest number of hydrophobic residues in contact with the solvent, the *O*−*P* dimer should be the most stable and the easiest to generate by protein engineering.

In the work presented here, several mutants across the *R*- and *Q*-axis interfaces of the GAPDH from *B. stearothermophilus* were generated, and their biochemical properties were investigated. Two different double mutations led to *O*−*P* dimers. Both dimeric GAPDHs were enzymatically inactive yet able to bind NAD and G3P or 1,3-dPG. In addition, both dimeric GAPDH mutants exhibited cooperativity in binding the coenzyme NAD. All these results are discussed in relation with the high-resolution three-dimensional structure of GAPDH from *B. stearothermophilus*.

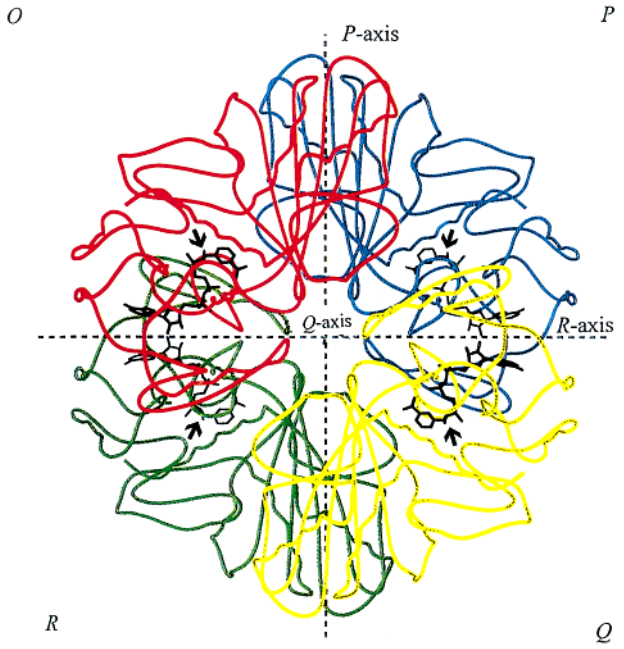


FIGURE 1: Spatial organization of the four subunits of the holo form of the GAPDH from *B. stearothermophilus* (*19*). Subunits *O*, *P*, *Q*, and *R* are represented by letters and colors red, blue, yellow, and green, respectively. Each colored line represents the main chain backbone of the subunit. Dashed lines represent the symmetry axes. The *Q*-axis is perpendicular to the plane of the paper. NAD is drawn in black lines. The arrow designates the S-loop.

## MATERIALS AND METHODS

*Molecular Modeling.* Molecular modeling was carried out on an INDIGO$^2$ Extreme Silicon Graphics workstation with the Brugel molecular modeling package version 10.1 (*22*). The crystallographic structure of the holo form of *B. stearothermophilus* GAPDH was taken from the Brookhaven Protein Data Bank (*23*), access code 1gd1.

*Site-Directed Mutagenesis.* Site-directed mutagenesis was performed using the method of Kunkel (*24*) on a pBluescript II SK containing the *gap* gene of *B. stearothermophilus* under the control of the *lac* promoter. The mutated genes were then sequenced to verify that no other mutation had arisen.

*Production and Purification of the Mutant GAPDHs of B. stearothermophilus.* Expression of GAPDH from *B. stearothermophilus* was carried out in *E. coli* strain HB101 as previously described (*25*). After sonication of the cell pellet, GAPDH was purified by ammonium sulfate fractionation (66−92%) and size-exclusion chromatography on ACA 34 resin equilibrated in 50 mM Tris/HCl (pH 8.0) containing 2 mM EDTA (buffer A). The resulting mixture of endogenous GADPH from *E. coli* and expressed GAPDH of *B. stearothermophilus* was separated on a Q-Sepharose FPLC column (Pharmacia), using a linear gradient from 0 to 200 mM KCl in buffer A.

*B. stearothermophilus* GAPDH was further purified on Phenyl-Sepharose (Pharmacia) equilibrated with buffer A,

[1] Abbreviations: GAPDH, phosphorylating glyceraldehyde-3-phosphate dehydrogenase; wtGAPDH, wild type glyceraldehyde-3-phosphate dehydrogenase; D-G3P, D-glyceraldehyde 3-phosphate; 1,3-dPG, 1,3-diphosphoglycerate; NAD, nicotinamide adenine dinucleotide (oxidized form); NADH, nicotinamide adenine dinucleotide (reduced form); $P_i$, inorganic phosphate; SDS−PAGE, polyacrylamide gel electrophoresis with sodium dodecyl sulfate; Tris, *N*-tris(hydroxymethyl)aminomethane.

containing 1.7 M $(NH_4)_2SO_4$. GAPDH was eluted with a linear gradient from 1.7 to 0 M $(NH_4)_2SO_4$ in buffer A, resulting in the homogeneous enzyme as verified by 10% SDS−PAGE (*26*). The molecular masses of all proteins were confirmed by mass spectrometry. The enzyme concentration was determined spectrophotometrically using absorption coefficients at 280 nm of $1.17 \times 10^5$ and $1.31 \times 10^5$ $M^{-1}$ $cm^{-1}$ for tetrameric apo and holo enzymes, respectively, to give the molar concentration of the oligomer (*10*, *27*). In the case of the dimeric apoenzyme, the value of $5.85 \times 10^4$ $M^{-1}$ $cm^{-1}$ was used.

*Enzyme Assays and Kinetics.* Initial rate measurements were carried out at 25 °C on a Kontron Uvikon 933 spectrophotometer by following the absorbance of NADH at 340 nm, as previously described (*25*). Data were fitted to the Michaelis−Menten equation using least-squares regression analysis to determine $k_{cat}$ and $K_M$. The turnover number ($k_{cat}$) was expressed per active site ($N$). All $K_M$ values were determined at saturating concentrations of all other substrates.

*Native Molecular Mass Determination.* Native molecular mass determination for mutant proteins was performed by gel filtration using a Superose 12 FPLC column (Pharmacia) equilibrated with buffer A containing 150 mM KCl, at a flow rate of 0.2 mL/min. For calibration, the following molecular mass standards (Bio-Rad) were used: (1) vitamin $B_{12}$ (1.35 kDa), (2) myoglobin (horse, 17.5 kDa), (3) ovalbumin (chicken, 44 kDa), (4) $\gamma$-globulin (beef, 158 kDa), and (5) tyroglobulin (670 kDa). The void and total volumes of the column, 6.9 and 18.2 mL, respectively, were determined with potassium bichromate and blue dextran dyes to enable calculation of the distribution coefficient $K_{av}$.

*Sucrose Density Gradient Centrifugation.* Gradients of 5 to 20% sucrose in buffer A with final volumes of 12 mL were set up in polyallomer tubes. Protein samples in buffer A were gently layered on top of the gradient. Centrifugation was performed with a Beckman L8-70M ultracentrifuge using a Beckman SW41 swing-bucket rotor (39 000 rpm for 24 h at 20 °C). Following centrifugation, 500 $\mu$L aliquots were withdrawn and the protein concentration was determined according to the Bradford procedure (*28*). Svedberg coefficients were calculated as previously described (*29*).

*Absorption Band of the Binary Enzyme−NAD Complex (Racker Band).* Measurements of the intensity of the absorption band, centered at 360 nm (*30*), were carried out as previously described (*31*). The temperature of the samples was maintained at 25 °C. The apoenzyme form of the wild type and Y46G, S48G, and E276G mutants was prepared by passage through an Affi-blue gel column (Bio-Rad) (*32*). Absorbance ratios ($OD_{280}/OD_{260}$) equal to 2 were obtained for wild type and mutant apoenzymes. The extinction of the absorption band by G3P (1 mM final concentration) or 1,3-dPG (0.5 mM final concentration) has been monitored as previously described (*33*).

*Spectrofluorometric Measurements.* Determination of NAD binding affinities at 25 °C was performed as previously described for the *E. coli* (*10*) and *B. stearothermophilus* (*11*) enzymes. In short, quenching of tryptophan fluorescence by NAD was used to monitor the binding of NAD to both wild type and mutant enzymes. Fluorescence measurements were performed with a SAFAS flx spectrofluorometer equipped with a mixing propeller. Excitation and emission wavelengths were set at 297 and 330 nm, respectively. Fluorescence intensities were corrected for the screening effect due to the absorption of NAD, for Raman emission by subtracting the buffer emission spectrum, and for additionnal quenching of fluorescence due to nonspecific binding of NAD to the enzyme at high concentrations of NAD. Assuming that changes in fluorescence follow closely the fraction of monomers saturated with NAD, we recalculated the data to give fractional saturation and free ligand concentration with the following equations:

$$\bar{Y} = \frac{F_0 - F_i}{F_0 - F_f}$$

and

$$N_f = N_t(1 - \bar{Y})$$

where $\bar{Y}$ is fractional saturation, $F_0$, $F_i$, and $F_f$ are the initial, current, and corrected (for the screening effect, Raman emission, and nonspecific binding of NAD) values of fluorescence, respectively, and $N_t$ and $N_f$ are the total and free concentration of NAD, respectively. The fractional saturation was directly fitted to the following equation to obtain values of microscopic dissociation constants for dimeric enzymes (*34*):

$$\bar{Y} \equiv \frac{\frac{2N_f}{K_1} + \frac{2N_f^2}{K_1K_2}}{1 + \frac{2N_f}{K_1} + \frac{N_f^2}{K_1K_2}}$$

The fractional saturation was also fitted to the logarithmic form of the Hill equation to obtain values for the Hill coefficient ($n$) and free NAD concentration at half-saturation ($N_{f0.5}$):

$$\log\left(\frac{\bar{Y}}{1 - \bar{Y}}\right) = n \times \log N_f - \log N_{f0.5}^{\ n}$$

The plot of $\log[\bar{Y}/(1 - \bar{Y})]$ versus $\log N_f$ is a straight line with a slope of $n$. When $\log[\bar{Y}/(1 - \bar{Y})] = 0$, the corresponding position on the $\log N_f$ axis gives $\log N_{f0.5}$. Both the Hill coefficient ($n$) and the ratio of the dissociation constants ($K_2/K_1$) measured the degree of cooperative interaction of the binding sites of the mutant in the study. There is negative, no, or positive cooperativity if $K_2/K_1 > 1$, $K_2/K_1 = 1$, or $K_2/K_1 < 1$, respectively. There is negative, no, or positive cooperativity if $n < 1$, $n = 1$, or $n > 1$, respectively. At the upper limit, $n$ is equal to 2.

## RESULTS

*Molecular Modeling.* A total of 26, 10, and 6 intersubunit hydrogen bonds are present in the *P*-axis, *R*-axis, and *Q*-axis interface, respectively (*19*). After careful examination of the three-dimensional structure (*19*, *20*), four interfacial hydrogen bond forming residues were selected among these 42 residues: Asp-186 and Ser-48, which are hydrogen bond partners across the *R*-axis interface, and Glu-276 and Tyr-46, which are hydrogen bond partners across the *Q*-axis interface (Table 1). These four residues share common properties. First, they are highly conserved among the

Table 1: Intersubunit Hydrogen Bonds Formed by Residues Asp-186 and Glu-276 of GAPDH from *B. stearothermophilus* As Described in ref *19*

| *R*-axis interface | | | | *Q*-axis interface | | | |
|---|---|---|---|---|---|---|---|
| Arg-13 | NH2 | Asp-186 | O | Glu-276 | OE2 | Lys-45 | NZ |
| Ser-48 | N | Asp-186 | OD2 | Glu-276 | OE2 | Tyr-46 | OH |
| Ser-48 | OG | Asp-186 | OD1 | Lys-45 | NZ | Glu-276 | OE2 |
| Asp-186 | OD2 | Ser-48 | N | Tyr-46 | OH | Glu-276 | OE2 |
| Asp-186 | OD1 | Ser-48 | OG | | | | |
| Asp-186 | O | Arg-13 | NH2 | | | | |

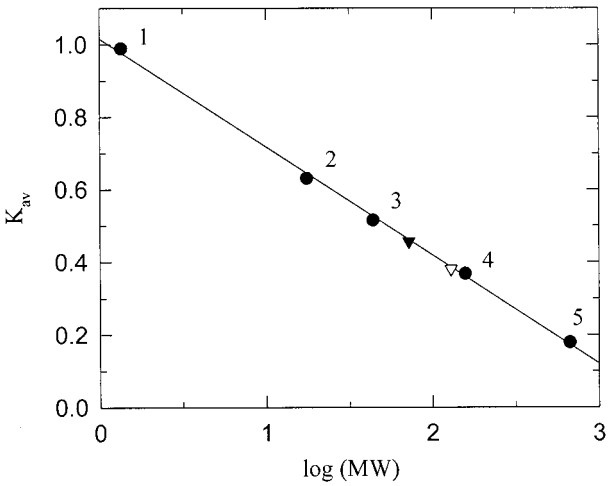


FIGURE 2: Molecular mass determination of mutant GAPDHs from *B. stearothermophilus* by gel filtration on Superose 12. Chromatography was performed at 0.2 mL/min in a Superose 12 FPLC column (Pharmacia) equilibrated with buffer A containing 150 mM KCl (see Materials and Methods). Molecular mass standards vitamin $B_{12}$, myoglobin, ovalbumin, $\gamma$-globulin, and tyroglobulin are represented (●) by a number from 1 to 5, respectively. Data for dimeric double mutants D186G/E276G and Y46G/S48G (▼) and tetrameric single mutants and wild type GAPDHs (▽) are also indicated.

GAPDHs from different species. Second, they all are located in loops. Tyr-46 and Ser-48 are located in the loop following helix $\alpha_c$, in the cofactor domain. Asp-186 is located in a loop called S-loop (*19*, *20*), which extends from residue 179 to 201, and Glu-276 is located in the loop following strand $\beta_5$, in the catalytic domain. All of the mentioned residues were replaced with glycine, which was expected to minimize conformational alterations of the loops.

*Purification and Characterization of the GAPDH Mutants.* All single and double mutants were expressed in *E. coli*, purified, and characterized. During the purification, the behavior of GAPDH mutants was similar to that of wtGAPDH except for the hydrophobic chromatography step. Dimeric and tetrameric enzymes were eluted with 200 and 600 mM ammonium sulfate, respectively. All mutant GAPDHs preserved secondary structure characteristics present in the wtGAPDH, judging by far-UV circular dichroism spectra (data not shown).

As expected, wtGAPDH was tetrameric. Under the experimental conditions, all GAPDH single mutants D186G, E276G, Y46G, and S48G were also tetrameric at as low an oligomer concentration as 0.1 $\mu$M. Molecular mass determination by size-exclusion chromatography using a Superose 12 column gave a similar $K_{av}$ of 0.38 for mutants and wtGAPDH (Figure 2) corresponding to a molecular mass of 129 ± 11 kDa, values in good agreement with the theoretical value of 144 kDa. Double mutants D186G/E276G and Y46G/S48G were dimeric for a dimer protein concentration of up to 350 $\mu$M, with a $K_{av}$ of 0.45 corresponding to a molecular mass of 72 ± 4 kDa (Figure 2). Centrifugation in sucrose density gradients confirmed the results of gel filtration experiments; Svedberg coefficients of 7.96 and 4.25 S were obtained for tetrameric and dimeric GAPDHs, respectively. Apo and holo forms of wtGAPDH were used as standards. Addition of coenzyme or one of the substrates did not change the oligomerization state of the enzymes: both double mutants D186G/E276G and Y46G/S48G remained dimeric even in the presence of a 50-fold excess of NAD or inorganic phosphate.

Table 2: Steady State Kinetic Parameters for Each Substrate of Mutant GAPDHs from *B. stearothermophilus*[a]

| | NAD $K_M$ (mM) | G3P $K_M$ (mM) | $P_i$ $K_M$ (mM) | $k_{cat}$ ($s^{-1}$) |
|---|---|---|---|---|
| wild type | 0.05 | 1.1 | 37 | 65 |
| D186G | 0.33 | 1 | 18 | 2 |
| E276G | 0.07 | 0.9 | 7 | 72 |
| D186G/E276G | | no detectable activity[b] | | |
| Y46G | 0.23 | 0.8 | 8 | 87 |
| S48G | 0.04 | 1 | 7 | 20 |
| Y46G/S48G | | no detectable activity[b] | | |

[a] The $k_{cat}$ and $K_M$ values were determined at saturating concentrations of all other substrates (see Materials and Methods) and expressed in terms of each subunit. The standard deviation is <20%. [b] No detectable activity means activity of $<10^{-3}$ $s^{-1}$.

*Kinetic Properties of the GAPDH Mutants.* Both single mutants D186G and E276G were enzymatically active with $K_M$ values for NAD of 0.33 and 0.07 mM, respectively. Activity of E276G was similar to that of the wild type, whereas Asp-186 substitution with a glycine resulted in a 32-fold decrease in the $k_{cat}$ (Table 2). Double mutant D186G/E276G was inactive under all the conditions that were employed, even at as high a dimer concentration as 40 $\mu$M. To investigate the result of mutations themselves on kinetic properties, we obtained and characterized variants of the hydrogen bond-partnered residues across *R*- and *Q*-axis interfaces. Single mutants Y46G and S48G led to active tetramers with $K_M$ values for NAD of 0.23 and 0.04 mM, respectively. The $k_{cat}$ of Y46G was similar to that of the wild type, while the $k_{cat}$ of S48G was only 3 times lower than that of the wild type enzyme. Double mutant Y46G/S48G led to an inactive dimer, like double mutant D186G/E276G. The fact that $K_M$ values for NAD of both single mutants D186G and Y46G are 6- and 5-fold greater than that for wtGAPDH, respectively, whereas values of microscopic dissociation constants $K_1$ and $K_2$ (see below) are lower than that of wtGAPDH, remains to be explained.

*NAD Binding to Wild Type and GAPDH Mutants.* The *B. stearothermophilus* GAPDH contains two tryptophan residues at positions 84 and 310 (*35*). Due to its positioning in the active site of the enzyme and on the basis of phosphorescence studies (*36*), Trp-310 is believed to be the higher emitting fluorescence probe. As reported previously (*11*), NAD binding resulted in quenching of the tryptophan fluorescence. UV−visible absorption and emission fluorescence spectra of native and mutant GAPDH apoenzymes were similar (curves not shown), and the maximum of the emission spectra corresponded to 330 nm. First, we studied NAD binding to dimeric mutants D186G/E276G and Y46G/

Table 3: NAD Microscopic Dissociation Constants of Wild Type and Mutant GAPDHs[a]

| | $K_1$ ($\mu$M) | $K_2$ ($\mu$M) | $K_2/K_1$ |
|---|---|---|---|
| wild type | 0.060 ± 0.014 | 0.25 ± 0.02 | 4 |
| D186G/E276G | 5.20 ± 0.43 | 1.51 ± 0.16 | 0.29 |
| Y46G/S48G | 5.54 ± 0.60 | 1.43 ± 0.14 | 0.26 |
| D186G | 0.040 ± 0.008 | 0.090 ± 0.001 | 2.25 |
| E276G | 0.052 ± 0.010 | 0.40 ± 0.08 | 8 |
| Y46G | 0.015 ± 0.002 | 0.12 ± 0.01 | 8 |
| S48G | 0.10 ± 0.01 | 0.13 ± 0.01 | 1.27 |

[a] Binding experiments and data analysis were performed as indicated in Materials and Methods. Microscopic dissociation constants were expressed as means ± standard deviations. The enzyme concentration was 2.70, 1.35, and 0.4 $\mu$M for wtGAPDH, dimeric double mutants, and tetrameric single mutants, respectively. The buffer was 50 mM Tris/HCl (pH 8.0).

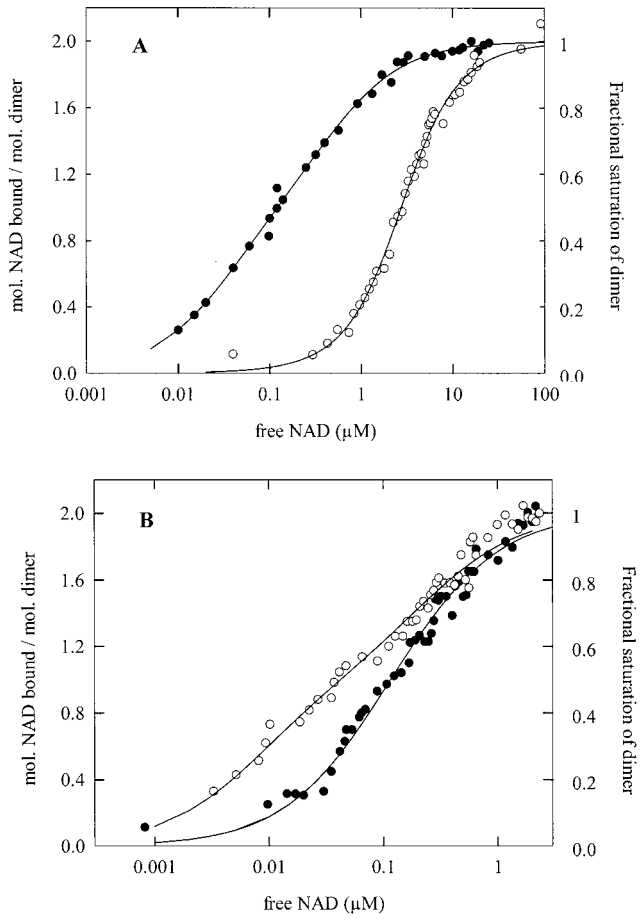


FIGURE 3: NAD binding curves of wild type and mutant GAPDHs. The molar ratio of NAD bound per mole of dimer was plotted against free NAD concentration, for the wild type and mutant enzymes. The corresponding value of fractional saturation of dimers ($\bar{Y}$) is indicated on the second *y*-axis. Experimental values were calculated from corresponding values of corrected fluorescence as indicated in Materials and Methods. Solid lines represent theoretical curves plotted with the dissociation constants listed in Table 3: (A) wild type enzyme (●) and dimeric double mutant D186G/E276G (○) and (B) tetrameric single mutants S48G (●) and Y46G (○).

S48G. For both dimers, NAD binding isotherms required at least two interacting binding sites for the best fit. Both dimeric mutants D186G/E276G and Y46G/S48G exhibited positive cooperativity for NAD binding with approximately the same $K_2/K_1$ of around 0.3 **(**Table 3 and Figure 3**)** and Hill coefficient of around 1.3 (Table 4 and Figure 4).

Table 4: Hill Coefficients and Free NAD Concentrations at Half-Saturation of Wild Type and Mutant GAPDHs[a]

| | Hill coefficient ($n$) | free NAD concentration at half-saturation ($N_{f0.5}$) |
|---|---|---|
| wild type | 0.66 ± 0.07 | 0.12 ± 0.02 |
| D186G/E276G | 1.28 ± 0.13 | 2.80 ± 0.30 |
| Y46G/S48G | 1.31 ± 0.15 | 2.80 ± 0.30 |
| D186G | 0.82 ± 0.08 | 0.06 ± 0.01 |
| E276G | 0.54 ± 0.07 | 0.14 ± 0.02 |
| Y46G | 0.53 ± 0.03 | 0.04 ± 0.01 |
| S48G | 0.94 ± 0.20 | 0.11 ± 0.01 |

[a] Binding experiment data are the same as those used in Table 3. Data analysis was performed as indicated in Materials and Methods. Hill coefficients and free NAD concentrations were expressed as means ± standard deviations.

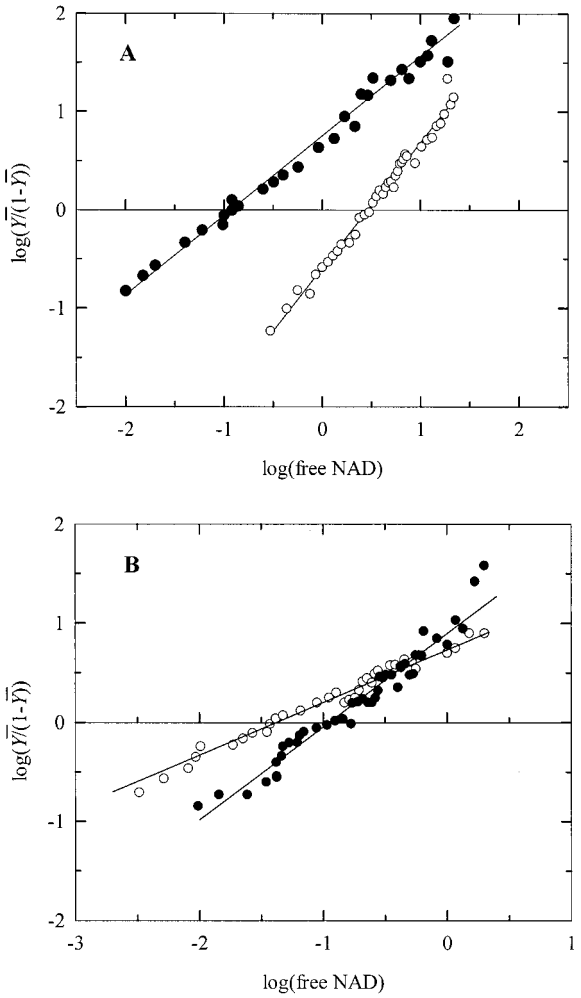


FIGURE 4: Hill plot of the NAD binding to wild type and mutant GAPDHs. The logarithmic form of the Hill equation, $\log[\bar{Y}/(1 - \bar{Y})]$ was plotted vs the logarithm of free NAD concentration. Experimental values were calculated from the corresponding available values of fractional saturation of dimers ($\bar{Y}$) and free NAD concentration. Solid lines represent theoretical curves plotted with Hill coefficients and free NAD concentrations at half-saturation listed in Table 4: (A) wild type enzyme (●) and dimeric double mutant D186G/E276G (○) and (B) tetrameric single mutants S48G (●) and Y46G (○).

Under the same experimental conditions, negative cooperativity was found for NAD binding to the tetrameric wtGAPDH, as previously reported (*11*). However, NAD binding to wtGAPDH could be adequatly described in terms of independent dimers with only two interacting binding sites

Table 5: Intensity of the Absorption Band, Centered at 360 nm, of the Binary Enzyme−NAD Complex[a]

| | $\epsilon_{360,monomer}$ of the binary enzyme−NAD complex ($M^{-1}$ $cm^{-1}$) |
|---|---|
| wild type | 1000 ± 75 |
| D186G | 892 ± 52 |
| E276G | 900 ± 45 |
| Y46G | 840 ± 37 |
| S48G | 870 ± 32 |
| D186G/E276G | 79 ± 9 |
| Y46G/S48G | 90 ± 11 |

[a] Differential spectroscopic measurements were carried out at 25 °C with two matched double-compartment cells. Enzyme concentrations were 80 $\mu$M in subunits for both tetrameric and dimeric GAPDHs.

(Table 3). This was also the case for all tetrameric single mutants. Tetrameric single mutants D186G, E276G, and Y46G exhibited negative cooperativity in binding the coenzyme NAD, while no significant cooperativity was detected for tetrameric single mutant S48G **(**Figures 3 and 4). Moreover, on the basis of the comparison of the $K_2/K_1$ ratios, negative cooperativity of Y46G and E276G mutants was more pronounced while that of the D186G mutant was less pronounced compared to that of the wild type enzyme. Hill coefficient values of GAPDH mutants were consistent with the degree of negative cooperativity deduced from the $K_2/K_1$ ratio (Table 4)**.** The fact that the S48G mutant did not exhibit significant cooperativity in binding the coenzyme NAD remained to be explained. The free NAD concentration at half-saturation ($N_{f0.5}$) deduced from a Hill plot is indicative of NAD affinity. The $N_{f0.5}$ values of D186G and Y46G mutants were 2- and 3-fold higher than that of the wild type, respectively, while those of the S48G and E276G mutants were similar to that of the wild type enzyme. The free NAD concentration at half-saturation for both dimeric mutants D186G/E276G and Y46G/S48G was 23-fold lower than for wtGAPDH.

*Absorption Band of the Binary Enzyme−NAD Complex.* The absorption band, centered at 360 nm, has been interpreted as a charge transfer between the positive charge of the pyridinium ring of NAD and the negative charge of the thiolate ion of essential Cys-149 (*30*). Its intensity is indicative of the relative positioning (distance and/or orientation) of the two moieties. Tetrameric mutants and wild type GAPDHs gave similar intensities of the absorption band under full saturation with NAD, whereas dimers exhibited a 10−12-fold lower intensity (Table 5). Addition of 1,3-dPG to all of the variant or wild type enzymes saturated with NAD led to a total disappearance of the absorption band. Addition of G3P to the binary enzyme−NAD complex resulted in disappearance of the absorption band for all dimeric GAPDHs. The latter could not be carried out with tetrameric enzymes because of the interference due to the formation of the NADH.

## DISCUSSION

Two models were used to describe both negative and positive cooperativity in GAPDHs. The preexisting asymmetry model is based on the asymmetry of the oligomeric enzyme and nonequivalent interactions between subunits. Cooperativity rises as a result of the preferential presence of both asymmetric and symmetric conformations and binding of the ligand to these conformations. The induced-fit model requires symmetric conformations for enzymes both unliganded and fully saturated with NAD enzymes, but allows asymmetric conformations for partially ligated enzyme. Ligand binding sequentially induces a conformational change of the bound subunit, giving rise to structural rearrangements of intersubunit contacts with the unliganded monomers and resulting in the observed cooperative effect. The interpretation of the crystallographic data obtained with lobster muscle GAPDH (*37*) showed potential asymmetry of the subunits, thus supporting the model with preexisting asymmetry. More recently, studies carried out with the insulin hexamer have demonstrated the applicability of this model (*38*). On the other hand, both crystallographic data (*17*, *19*, *20*) and studies in solution (*11*, *12*) supported the induced-fit model in the case of GAPDH from *B. stearothermophilus.* Indeed, no asymmetry was detected either in the apoenzyme or in the holoenzyme in high-resolution three-dimensional structures of the GAPDH from *B. stearothermophilus* (*19*, *20*). In addition, the tetramer with NAD ligated in a single subunit preserved a conformation very similar to that of the apoenzyme in the unliganded subunits, while the structure of the NAD-bound subunit was almost identical to that of the holoenzyme subunit (*17*). Therefore, we based our analysis of binding data for GAPDH from *B. stearothermophilus* on an induced-fit model.

In the study presented here, we examined the biochemical and catalytic properties of tetrameric and dimeric GAPDH mutants from *B. stearothermophilus* to shed more light on the nature of the intersubunit interactions involved in cooperativity and activity. Detailed analysis of NAD binding to wtGAPDH revealed that this enzyme could be described by a minimum of two dissociation constants. This led us to conclude that the tetramer wtGAPDH consists of two independent NAD binding dimers, as if they were separated in space. This conclusion, combined with the induced-fit model, means that in the free enzyme, all subunits exist in the same conformation. Binding of NAD to one subunit changes the conformation of the neighboring subunit in the same dimer, yet leaves another dimer with an unchanged conformation. All other tetrameric variant GAPDHs, except S48G that did not exhibit significant cooperativity, possessed varied degrees of negative cooperativity in NAD binding and also required a minimum of two dissociation constants to describe the data.

This is not necessarily in contradiction with the previous study (*11*), which determined four dissociation constants for wtGAPDH. It is well accepted that if the data can be described with an equation, then any equation with greater complexity will also describe the data with the same goodness of fit, but with somewhat higher deviations in parameter values. Three out of four constants in the previously published study were characterized with high standard deviations. Moreover, all three of them gave the same microscopic dissociation constant value of 0.29−0.33 $\mu$M. This led us to the conclusion that three out of four dissociation constants are redundant, and tetrameric wtGAPDH can be described as two independent dimers with two interacting binding sites in each of the dimers. This is not in contradiction with the three-dimensional structure of the GAPDH from *B. stearothermophilus* which is described as a dimer of dimers (*19*, *20*).

Both dimeric double mutants D186G/E276G and Y46G/S48G exhibited positive cooperativity in NAD binding. The fact that dimeric double mutants retain cooperative behavior indicated that the *O*−*P* dimer is most probably the dimer that is responsible for the NAD binding cooperativity in tetrameric enzymes. As a consequence, we concluded that, first, the *P*-axis interface is essential to transmission of the structural information induced by NAD binding from one subunit to another and, second, the S-loop of the *R*-axis-related subunit is not directly involved in NAD binding cooperativity. These conclusions confirm previous observations, which indicate that the S-loop is rigidly maintained within the tetramer core having the same conformation in the apo- and holoenzyme (*21*). These results also support a previous assumption that the conformational changes induced upon NAD binding to the first subunit are transmitted through the *P*-axis interface from the external strands of the $\beta$-sheet of one subunit to the external strands of the catalytic domain $\beta$-sheet of the *P*-axis-related subunit (*21*). However, the nature of the mutations could modulate the NAD binding cooperativity of the dimer, as confirmed by another *O*−*P* dimer recently generated by double mutation (N180G/E276G) which exhibited negative cooperativity for NAD binding (O. Roitel, unpublished results). The reasons for the different cooperative behaviors of the wild type enzyme and tetrameric and dimeric mutants remained to be elucidated on the structural level.

Comparison of $K_2/K_1$ ratios for single mutants showed that residues Ser-48 and Asp-186 are more important for revealing negative cooperativity than residues Tyr-46 and Glu-276. Both pairs are the natural hydrogen bond partners in the wild type enzyme. In addition, mutation of either Ser-48 or Asp-186 resulted in decreased activity, whereas substitution of Tyr-46 and Glu-276 residues led to a slightly increased catalytic efficiency. On the basis of this observation, we conclude that the *P*-axis interface determines cooperativity of the *O*−*P* or *Q*−*R* dimers. However, our studies cannot exclude the possibility that interactions with the neighboring dimer can also stabilize the subunit in an optimal conformation and thus participate in revealing cooperativity.

In tetrameric wtGAPDH, NAD is embedded in a cavity composed of residues from the cofactor domain (residues 1−148 and 312−333), of the N-terminal part of the S-loop of the same subunit (residues 178−182), and of the C-terminal part of the S-loop (residues 186−196) from the *R*-axis-related subunit. In the *O*−*P* dimer, the interaction of the S-loop with the active site of the *R*-axis-related subunit is disrupted, and the S-loop is presumably less structured. This hydrophobic loop is now exposed to the solvent with a subsequent increase in the hydrophobic character of the dimers, as confirmed by hydrophobic chromatography. In the dimers, accessibility of the active site to solvent should be increased, particularly for the adenosine-binding site of NAD. This may explain, first, the lower affinity of the dimeric enzyme for NAD and, second, the suboptimal positioning of the pyridinium ring relative to the thiolate ion of the essential Cys-149, as indicated by the lower intensity of the Racker band. Similar to our results, the N313T mutant of *E. coli* GAPDH has a suboptimal positioning of the pyridinium ring of NAD relative to the essential thiolate group (*21*), and the mutation did not eliminate cooperativity in NAD binding (*10*). In the case of *O*−*P* dimers of *B. stearothermophilus* GADPH, the absorption band of the binary enzyme−NAD complex disappeared after addition of 1,3-dPG or G3P, indicating that a covalent complex between the holoenzyme and G3P or 1,3-dPG was likely formed. However, the absence of catalytic activity demonstrated that these ternary complexes were not catalytically efficient.

Both double mutants D186G/E276G and Y46G/S48G were inactive, whereas all single mutants retained activity. This suggests that the absence of activity is due to the suboptimal position of the S-loop and not due to any single mutation. This has been recently supported by the fact that mutation of Arg-197, which is an intrasubunit hydrogen bond partner of Asp-186 (*19*), to glycine has also led to a mutant GAPDH with very low activity (O. Roitel, unpublished results). Moreover, the suboptimal position of the S-loop should also perturb the efficient positioning of at least three key residues, namely, Thr-179 and Arg-195, which are part of the G3P and $P_i$ binding sites, respectively, and Asn-180, which is involved in NAD binding (*20*). Also, we cannot exclude the possibility of a feasible interaction of the S-loop with the exposed hydrophobic core of the dimer, thus resulting in an unnatural conformation of a corresponding dimer in the tetramer. To discount these explanations, it would be necessary to generate an *O*−*P* dimer with a stabilized S-loop having the same conformation as it has in the tetramer and with an adenosine subsite having the same solvent accessibility as in the tetramer.

## ACKNOWLEDGMENT

We are very grateful to Dr. N. Zorn, Dr. H. Rogniaux, and Dr. A. Van Dorsselaer for determining the molecular masses of wild type and mutant GAPDHs and to Dr. E. Duée for helpful discussions. We thank the Service Commun de Biophysicochimie of the University Henri Poincaré Nancy I for allowing us to perform the molecular modeling studies. We also thank E. Habermacher, S. Boutserin, and S. Azza for their very efficient technical help.

## REFERENCES

1. Traut, T. W. (1994) *Crit. Rev. Biochem. Mol. Biol. 29*, 125−163.
2. Klotz, I. M., Darnall, D. W., and Langerman, N. R. (1975) in *The Proteins* (Neurath, H., and Hill, R. L., Eds.) pp 293−411, Academic Press, New York.
3. Goodsell, D. S., and Olson, A. J. (1993) *Trends Biochem. Sci. 18*, 65−68.
4. Kirschner, K., Gallego, E., Schuster, I., and Goodall, D. (1971) *J. Mol. Biol. 58*, 29−50.
5. Conway, A., and Khosland, D. E. (1968) *Biochemistry 7*, 4011−4022.
6. Boers, W., Oosthuizen, C., and Slater, E. C. (1971) *Biochim. Biophys. Acta 250*, 35−46.
7. Seydoux, F., Bernhard, S., Pfenninger, O., Payne, M., and Malhotra, O. P. (1973) *Biochemistry 12*, 4290−4300.
8. Kelemen, N., Kellershohn, N., and Seydoux, F. (1975) *Eur. J. Biochem. 57*, 69−78.
9. De Wildjer, J. J. M., Boers, W., and Slater, E. C. (1969) *Biochim. Biophys. Acta 191*, 214−220.
10. Corbier, C., Mougin, A., Mely, Y., Adolph, H. W., Zeppezauer, M., Gerard, D., Wonacott, A., and Branlant, G. (1990) *Biochimie 72*, 545−554.
11. Clermont, S., Corbier, C., Mely, Y., Gerard, D., Wonacott, A. J., and Branlant, G. (1993) *Biochemistry 32*, 10178−10184.

12. Allen, G., and Harris, J. I. (1975) *Biochem. J. 151*, 747−749.
13. Monod, J., Wyman, J., and Changeux, J. P. (1965) *J. Mol. Biol. 12*, 88−118.
14. Malhotra, O. P., and Bernhard, A. (1968) *J. Biol. Chem. 243*, 1243−1252.
15. Malhotra, O. P., and Bernhard, A. (1973) *Proc. Natl. Acad. Sci. U.S.A. 70*, 2077−2081.
16. Khosland, D. E., Nemethy, G., and Filmer, D. (1966) *Biochemistry 5*, 365−384.
17. Leslie, A. G. W., and Wonacott, A. J. (1983) *J. Mol. Biol. 165*, 375−391.
18. Harris, J. I., and Waters, M. (1976) in *The Enzymes* (Boyer, P. D., Ed.) Vol. 13, pp 1−49, Academic Press, New York.
19. Skarzynski, T., Moody, P. C., and Wonacott, A. J. (1987) *J. Mol. Biol. 193*, 171−187.
20. Skarzynski, T., and Wonacott, A. J. (1988) *J. Mol. Biol. 203*, 1097−1118.
21. Duée, E., Olivier-Deyris, L., Fanchon, E., Corbier, C., Branlant, G., and Dideberg, O. (1996) *J. Mol. Biol. 257*, 814−838.
22. Delhaise, P., Bardiaux, M., and Wodak, S. J. (1984) *J. Mol. Graphics 2*, 103−106.
23. Bernstein, F. C., Koetzle, T. F., William, G. J. B., Meyer, E. F., Brice, M. D., Rodgers, J. R., Kennard, O., Shimanouchi, T., and Tasumi, M. (1977) *J. Mol. Biol. 112*, 535−542.
24. Kunkel, T. A., Bebenek, K., and McClary, J. (1991) *Methods Enzymol. 204*, 125−139.
25. Mougin, A., Corbier, C., Soukri, A., Wonacott, A., Branlant, C., and Branlant, G. (1988) *Protein Eng. 2*, 45−48.
26. Laemmli, U. K. (1970) *Nature 227*, 680−685.
27. Corbier, C., Clermont, S., Billard, P., Skarzynski, T., Branlant, C., Wonacott, A., and Branlant, G. (1990) *Biochemistry 29*, 7101−7106.
28. Bradford, M. M. (1976) *Anal. Biochem. 72*, 248−254.
29. Stancel, G. M., and Gorski, J. (1975) *Methods Enzymol. 36*, 166−176.
30. Racker, E., and Krimsky, I. (1952) *J. Biol. Chem. 198*, 731−743.
31. Soukri, A., Mougin, A., Corbier, C., Wonacott, A., Branlant, C., and Branlant, G. (1989) *Biochemistry 28*, 2586−2592.
32. Talfournier, F., Colloc'h, N., Mornon, J. P., and Branlant, G. (1998) *Eur. J. Biochem. 252*, 447−457.
33. Harrigan, P. J., and Trentham, D. R. (1973) *Biochem. J. 135*, 695−703.
34. Adair, G. S. (1925) *J. Biol. Chem. 63*, 529−545.
35. Branlant, C., Oster, T., and Branlant, G. (1989) *Gene 75*, 145−155.
36. Gabellieri, E., Rahuel-Clermont, S., Branlant, G., and Strambini, G. B. (1996) *Biochemistry 35*, 12549−15559.
37. Moras, D., Olsen, K. W., Sabesan, M. N., Buehner, M., Ford, G. C., and Rossmann, M. G. (1975) *J. Biol. Chem. 250*, 9137−9162.
38. Bloom, C. R., Kaarsholm, N. C., Ha, J., and Dunn, M. F. (1997) *Biochemistry 36*, 12759−12765.

BI9912802